# Vibrational dynamics in liquids and frozen matrices. Concentration and solvent effects in phenylacetylene by low temperature Raman spectroscopy

B. Brożek, H. Abramczyk *

*Technical University, Institute of Applied Radiation Chemistry, Wróblewskiego 15 street, 93-590 Łódź, Poland*

Received 10 May 1999; in final form 12 August 1999

## Abstract

Raman spectra of the $\nu_s(C\equiv C)$ stretching mode of phenylacetylene (PA) dissolved in different solvents: methylcyclohexane, acetonitrile and benzene in frozen matrices at 77 K as a function of concentration have been recorded and compared with the spectra in the liquid phase. The optical measurements were complemented by the differential scanning calorimetry (DSC) scans. The results reveal some dramatic changes with solvent and concentration and are of potential relevance both to fundamental condensed phase modelling and to liquid crystal technology. We have discussed the origin of the splitting observed for the $\nu_s(C\equiv C)$ stretching mode of phenylacetylene (PA) and we have found that H-bond interactions are responsible for the observed substructure in the vibrational spectra. We have found a glass-like transition at 183 K and two melting-like transitions at 200 and 218 K for PA in acetonitrile. In methylcyclohexane a melting transition starts at 120 K, and does not change in PA solution in contrast to PA in acetonitrile. The DSC scan for PA in methylcyclohexane shows additional phase transition at about 220 K. © 1999 Elsevier Science B.V. All rights reserved.

## 1. Introduction

Various aspects of glass-forming liquids, and in particular, the transitions between the glass and supercooled liquid states of condensed matter has become a significant topic in modern chemistry [1]. Temperature-dependent studies in a broad temperature range will become increasingly important because allows to monitor dynamics in systems of diverse morphology and to determine the general behaviour of liquids, liquid crystals, and glasses near their phase transitions.

Phenylacetylene derivatives have attracted much attention because of their unique properties used in the most recent liquid crystal technologies to achieve high-purity nematic materials [2]. The acetylene linkage $X–C\equiv C–Y$ which plays a role of a conjugative linking group between the core units provides the nematic phase stability much higher than in the parent cyanobiphenyls, well-known nematogenics, the first commercially available liquid crystals. Liquid crystal properties are strongly modified by solvent or host matrix and have become a subject to extensive studies because of possible applications in display technologies including polymer-dispersed liquid crystals (PDLCs) and other confined geometries formed by polymer and porous networks [2].

* Corresponding author. Fax: +48-42-360246; e-mail: abramczy@mitr.p.lodz.pl

The modified morphology of these systems, which is strongly solvent-, temperature- and concentration-dependent, leads to materials of different properties from isotropic liquids, crystalline or polycrystalline solids, plastic crystals to polyamorphic glasses and amorphous glasses. There is a need to distinguish between the different phases and to find how these forms coexist, because the polymorphism leads to striking changes in optical properties and disturbs response of liquid crystal materials to an electric field, which are important characteristics industry deals with.

Raman spectroscopy is a very powerful optical method in the study of changes in intermolecular structure that accompany transitions from isotropic liquids to crystalline or glassy solid phases and it is able to monitor the changes around vibrational oscillators at the molecular level. Differential scanning calorimetry (DSC), which complements optical methods in our paper is a useful tool, but in contrast to Raman spectroscopy it detects the enthalpy changes associated with each phase transition and the precise identity of any molecular parameters cannot be obtained.

It will be very important to extend the existing studies on vibrational dynamical and static properties to a wider temperature range in order eventually to develop an understanding of the relation between vibrational dynamics and phase transitions like liquid–crystal, liquid–glass, liquid–liquid crystal transitions at the molecular level and to learn what is universal in such relations.

A great deal of work is still needed to establish such connections. One of the goals of the proposed work is to develop such connections through systematic spectroscopic studies on temperature, solvent, and concentration effects. In this paper we will focus on the symmetric stretching mode of the triple bond C≡C of phenylacetylene studying the concentration effect in methylcyclohexane, acetonitrile and benzene at 77 K. The optical Raman spectra were complemented by the differential scanning calorimetry (DSC) measurements. The solvents were chosen because of their different behaviour in solid phases. Nonpolar methylcyclohexane and polar acetonitrile belong to 'floppy' molecules because of the presence of the methyl group which is less rigid than the aromatic rings, and this feature may lead to more pronounced delocalization at low temperatures. On the other hand, neat methylcyclohexane forms a glassy state in contrast to neat acetonitrile and benzene, which belong to crystalline materials.

To our knowledge the thermodynamic and optical behaviour of PA in these solvents at low temperatures are unknown and reported in this paper for the first time.

## 2. Experiment

Spectrograde methylcyclohexane, acetonitrile, benzene and phenylacetylene were purchased from Aldrich. Methylcyclohexane, acetonitrile, benzene were used without further purification. Phenylacetylene was destillated under vacuum before preparing solutions. Raman spectra were measured with Ramanor U1000 (Jobin Yvon) and Spectra Physics 2017-04S argon ion laser operating at 514 nm. The band corresponding to the C≡C stretching mode of PA in methylcyclohexane, acetonitrile, benzene was measured at 77 K. The spectral slit width was 1.3 cm$^{-1}$, which corresponds to the 200 $\mu$m mechanical slit of the spectrometer. We have calculated the widths after the deconvolution procedure corrected for finite slit width according to the formula [3]

$$\Delta_{1/2}^{t} = \Delta_{1/2}^{a}\left(1 - 2\left(s/\Delta_{1/2}^{a}\right)^{2}\right)^{1/2}, \qquad (1)$$

where $\Delta_{1/2}^{t}$ and $\Delta_{1/2}^{a}$ denote the band width after the deconvolution and the experimental band width, respectively, $s$ is the spectral slit width.

For very narrow Raman bands at 77 K it may happen that the formula (1) cannot be applied. In these cases we subtract the slit widths from the total band width $\Delta_{1/2}^{a}$, which is justified as both the instrumental and the experimental lines at 77 K are close to Lorentzians shapes at low temperatures.

The signal to noise ratio in liquid solutions is about 70:1. Similar ratio is observed in frozen matrices at higher concentration of PA whereas at lower concentrations the ratio is lower being about 20:1 in the worst cases. The smaller ratios come from the fact that measurements in cryostat give always lower intensities of the signals than in the standard liquid couvette and going to lower temperatures the intensity decreases drastically at around 200 K in comparison with the liquid phase. Spectra were recorded at

room temperatures, and at 77 K in a liquid nitrogen bath cryostat. The samples at 77 K were prepared in two different ways: by rapid quenching with sudden immersing the sample in liquid nitrogen and by slow cooling with temperature going down gradually at the average cooling rate of 0.5°C/min. The samples were cooled in commercial glass ampoules of approximately 1 cm diameter and 1 ml solution volume. The samples at 293 K are transparent while the samples at 77 K are much more opaque although a small part of the laser beam penetrates the whole length of the sample.

A polarization analyser and $\lambda/4$ waveplate were used to select VV and VH components. The isotropic Raman spectra were calculated according to the relation

$$I_{\mathrm{iso}} = I_{\mathrm{VV}} - \tfrac{4}{3} I_{\mathrm{VH}} . \qquad (2)$$

The depolarization ratio defined as

$$\rho = \frac{I_{\mathrm{VH}}}{I_{\mathrm{VV}}} , \qquad (3)$$

was measured for each sample.

The interference filter has been used to purify the laser line by removing additional natural emission lines which interfere with the Raman lines, especially in the case of solid samples.

Differential scanning calorimetry traces were measured during the heating at 1 atm pressure with Netzsch DSC 200 instrument in samples of 80 mg in the temperature range from 143 to 298 K.

## 3. Results and discussion

Fig. 1 shows the Raman (VV component) band shapes of the stretching mode $\nu_{\mathrm{s}}(\mathrm{C}\equiv\mathrm{C})$ as a function of PA concentration in methylcyclohexane at 77 K.

Fig. 2 shows the Raman band shapes (VV component) of the stretching mode $\nu_{\mathrm{s}}(\mathrm{C}\equiv\mathrm{C})$ as a function of PA concentration in acetonitrile at 77 K.

For comparison, Fig. 3 shows the Raman band shapes (VV component) of the stretching mode $\nu_{\mathrm{s}}(\mathrm{C}\equiv\mathrm{C})$ as a function of PA concentration in benzene at 77 K [4]. The VH Raman components and the Raman spectra obtained without the polarization analyzer are similar in their character to the VV components. The isotropic Raman components at higher temperatures are also similar to the VV and
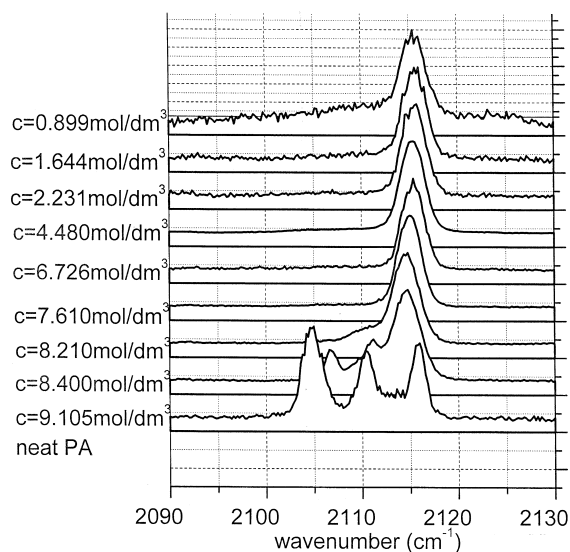


Fig. 1. VV Raman spectra of the C≡C stretching mode of phenylacetylene in methylcyclohexane as a function of concentration at 77 K (rapid cooling).

VH spectra, but at around 200 K the isotropic component suddenly disappears.

The results presented in Figs. 1–3 illustrate how important role is played by the solvent at low temperatures. Indeed, Figs. 1–3 show three different systems, which consist of essentially the same vibration of the acetylene (C≡C) linkage of phenylacetylene immersed in three different environments: methylcyclohexane, acetonitrile and benzene. Evidently different behaviour has been found in various environments at 77 K. It is worth emphasising that the spectra of the samples prior to the quench show slightly asymmetric on the low frequency side, broad, structureless band. Compared to the results over the equilibrium liquid range [5,6], where the band shapes are similar in all the solvents, and the samples show no miscibility problems in the full concentration range, the systems at 77 K demonstrate spectacular change depending on solvent properties at low temperatures. In methylcyclohexane, a single narrow peak at about 2116 cm$^{-1}$ is observed up to PA concentration around $c = 8.21$ mol/dm$^3$. For higher PA concentration the additional two peaks at 2105 and 2110 cm$^{-1}$ begin to reveal, which become clearly evident for PA concentration $c = 9.105$ mol/dm$^3$, which corresponds to neat PA. In con-
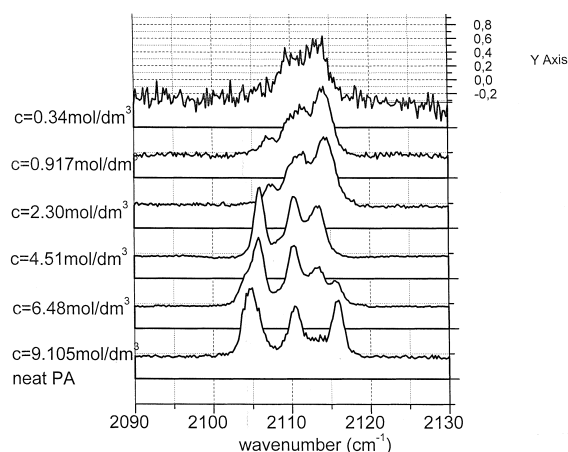
Fig. 2. VV Raman spectra of the C≡C stretching mode of phenylacetylene in acetonitrile as a function of concentration at 77 K (rapid cooling).

trast, for PA in acetonitrile the vibrational substructure can be seen for all PA concentration starting from $c = 0.34$ up to 9.105 mol/dm$^3$ with the three peaks at 2105, 2110 and 2116 cm$^{-1}$, respectively. The most spectacular changes with increasing PA concentration have been found for PA in benzene at 77 K (Fig. 3) [4]. At lower PA concentrations ($c = 0.372$–0.927 mol/dm$^3$) we observe a single narrow peak with the maximum at about 2116 cm$^{-1}$. At higher concentrations ($c = 1.753$–3.44 mol/dm$^3$) the

bands still remain narrow with the maximum at 2116 cm$^{-1}$. At higher concentrations the intensity at the low frequency side of the band begins to increase resulting in significant band broadening in the PA concentration range between $c = 4.604$ to 7.949 mol/dm$^3$ similar to that found in the liquid phase. For further increasing PA concentration the broad band begins to split into three peaks.

It is evident that the changes observed in the Raman band profiles and band widths with concentration must illustrate the changes of the mechanisms of vibrational dynamics due to structural reorganisation or phase transitions. Moreover, the results presented here show that the Raman spectra of PA in solutions depend on the rate of quenching. The results presented in Figs. 1–3 were obtained for the case of rapid cooling by immersing the sample into liquid nitrogen at 77 K.

In Figs. 4–6 we present the results for the same systems but the samples were quenched slowly at the cooling rate of 0.5°C/min with gradual temperature decreasing going from 298 down to 77 K. We can see remarkable differences in the band profiles for the case of rapid and slow cooling. The most spectacular changes are observed for PA in benzene (Figs. 3 and 6). In contrast to the single peak at 2116 cm$^{-1}$ observed for lower PA concentrations for rapid cooling (Fig. 3) we can see the sharp peak on the red side at 2105 cm$^{-1}$ accompanied by two additional
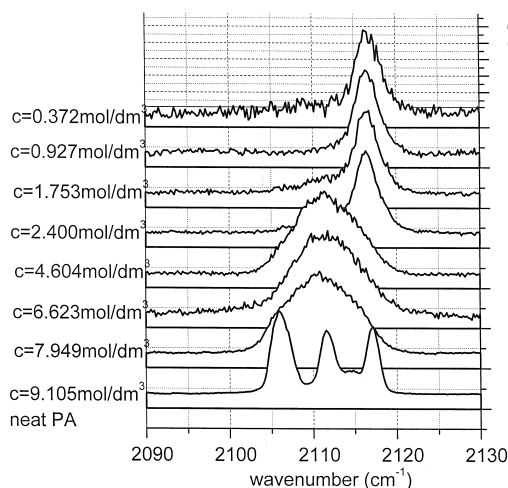


Fig. 3. VV Raman spectra of the C≡C stretching mode of phenylacetylene in benzene as a function of concentration at 77 K (rapid cooling) [4].
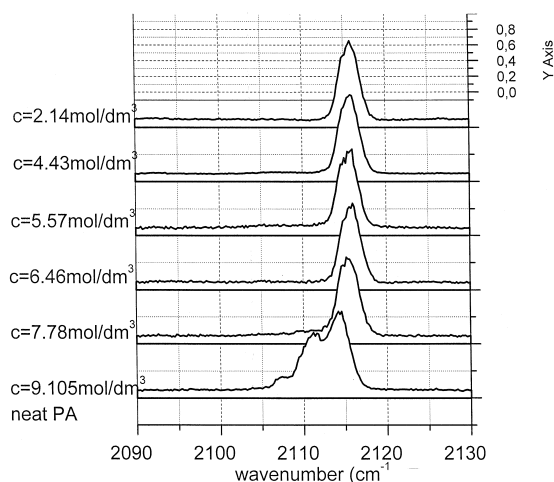


Fig. 4. VV Raman spectra of the C≡C stretching mode of phenylacetylene in methylcyclohexane as a function of concentration at 77 K (slow cooling).
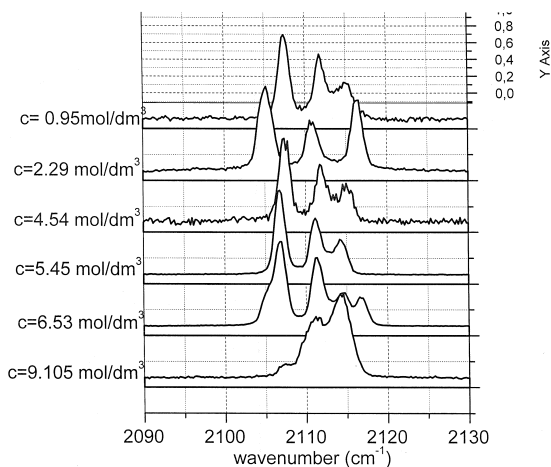
Fig. 5. VV Raman spectra of the C≡C stretching mode of phenylacetylene in acetonitrile as a function of concentration at 77 K (slow cooling).

peaks of smaller intensity at 2110 and 2116 cm$^{-1}$ for slow cooling (Fig. 6). As PA concentration increases the intensity of the peak at 2105 cm$^{-1}$ decreases with simultaneous intensity increase of the peaks at 2110 and 2116 cm$^{-1}$. The differences between the band profiles of PA in methylcyclohexane (Figs. 1 and 4) and acetonitrile (Figs. 2 and 5) for rapid and slow cooling are less spectacular but also remarkable. For rapid cooling (Fig. 2) and lower PA concentrations (0.34–2.3 mol/dm$^3$) the intensity of the peak at 2105 cm$^{-1}$ for PA in acetonitrile is small and becomes to increase with PA concentration, in contrast to the case of slow cooling (Fig. 5) where the intensity of the peak at 2105 cm$^{-1}$ begins to decrease with PA concentration.

To ascertain what happens to vibrational relaxation channels, which are reflected by the rather dramatic and sudden changes in the spectral lineshapes and to answer how universal or specific the results for PA in solutions are, we should know more about the thermodynamic states of PA in solutions. After optical method, the material should be examined by DSC method to check the phase transitions and hopefully to lead to the likely identity of the mesophases.

Figs. 7 and 8 show a differential scanning calorimeter scan of neat acetonitrile and PA in acetonitrile at nearly the same concentration ($c = 0.91$ mol/dm$^3$) as for the Raman spectra. The phase

diagram for PA in acetonitrile shows a glass-like transition at 183 K (revealed by a slight inflection in the baseline on the DSC trace) followed by two melting-like endotherms at 200 and 218 K. Comparing Fig. 7 with Fig. 8 shows a striking difference between neat acetonitrile and PA in acetonitrile in the region of a melting transition. We can see that not only the melting point has depressed from around 230 to around 200 K but also an additional DSC melting-like peak has appeared at around 218 K. This additional peak is barely detectable in the DSC trace of neat acetonitrile. In PA solution both peaks are of comparable magnitude and it is hard to believe that the first peak at 200 K represents the melting transition from a solid to a liquid crystal followed by a liquid crystal to liquid crystal or a liquid crystal to isotropic liquid transition at around 218 K as the latter transitions are known to be characterised by very much smaller enthalpy changes. The DSC changes similar to that we observed in PA–acetonitrile system have been reported in literature for plastic crystals [7], which undergo a solid–solid phase transition below the melting point. The solid–state transition in plastic crystals exhibits a large entropy change comparable to or even greater than during the solid–liquid transition. Taking into account the similarity of the DSC scans and a waxy appearance and plastic consistency around melting of pure pheny-
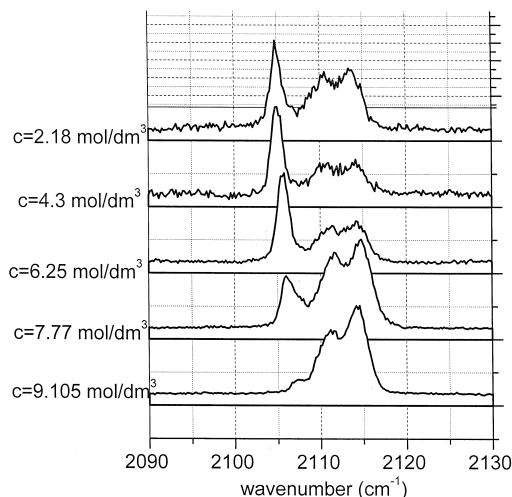


Fig. 6. VV Raman spectra of the C≡C stretching mode of phenylacetylene in benzene as a function of concentration at 77 K (slow cooling) [4].
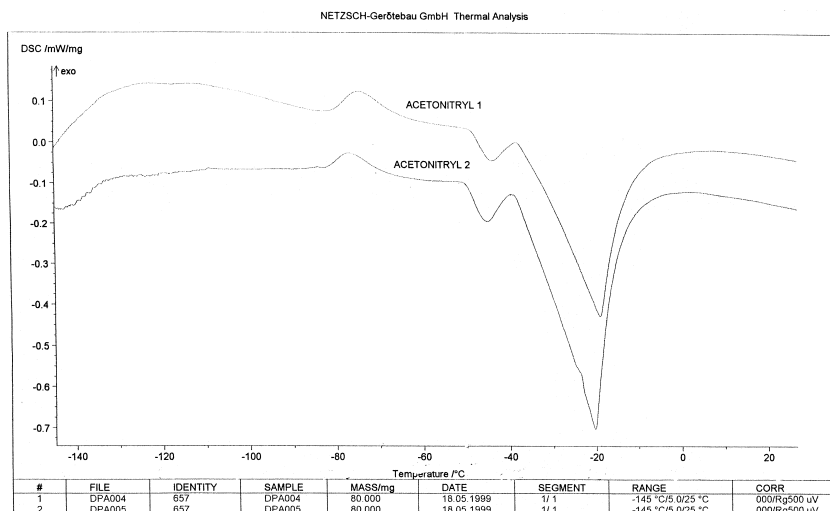
NETZSCH-Gerätebau GmbH  Thermal Analysis

Fig. 7. Differential scanning calorimeter scan of neat acetonitrile.

lacetylene, we ascribed the transition at 183 K to the crystal–plastic crystal transition, the plastic crystal–glassy plastic crystal transition at 200 K and the glassy plastic crystal–liquid phase transition at 218 K. A detailed understanding is required of molecular motions that occurs during the course of the phase transitions and which degrees of freedom melt at the transitions from the ordered to the disordered structures. Although the orientational disorder provides a

very appealing route to a description of the plastic crystals properities [7], we would like to emphasise the role which can be played by H-bond interactions on translational and orientational rigidity for studied in this paper systems.

A more illuminating picture to the elucidation of origin of the phase transitions monitored by the DSC traces for PA solutions comes from the comparison of the DSC traces for neat acetonitrile and PA in

NETZSCH-Gerätebau GmbH  Thermal Analysis
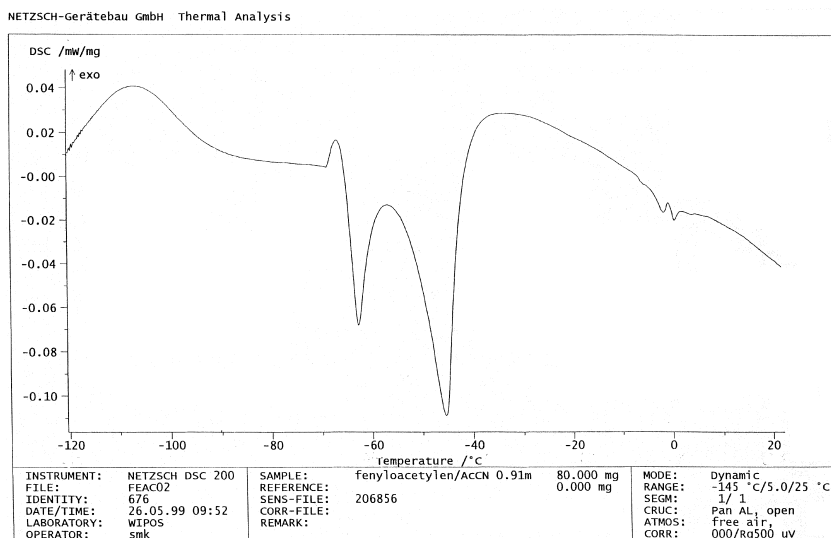
Fig. 8. Differential scanning calorimeter scan of phenylacetylene in acetonitrile (0.91 mol/dm$^3$).
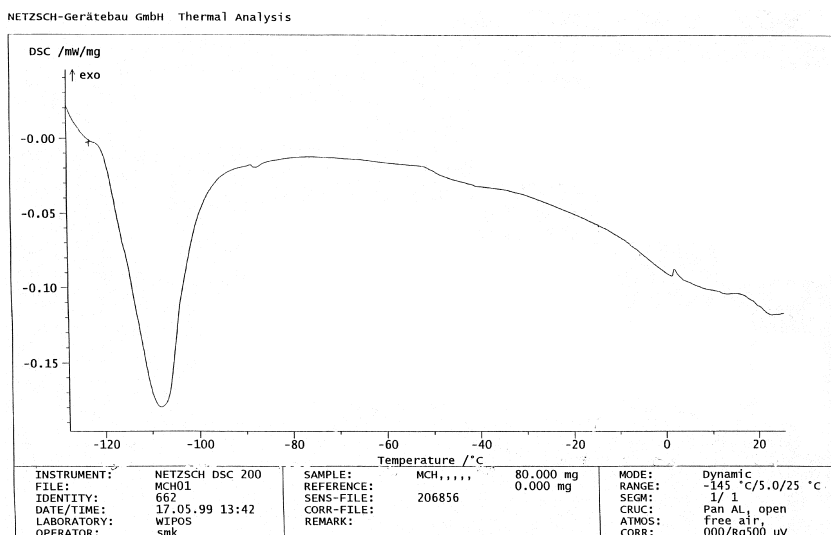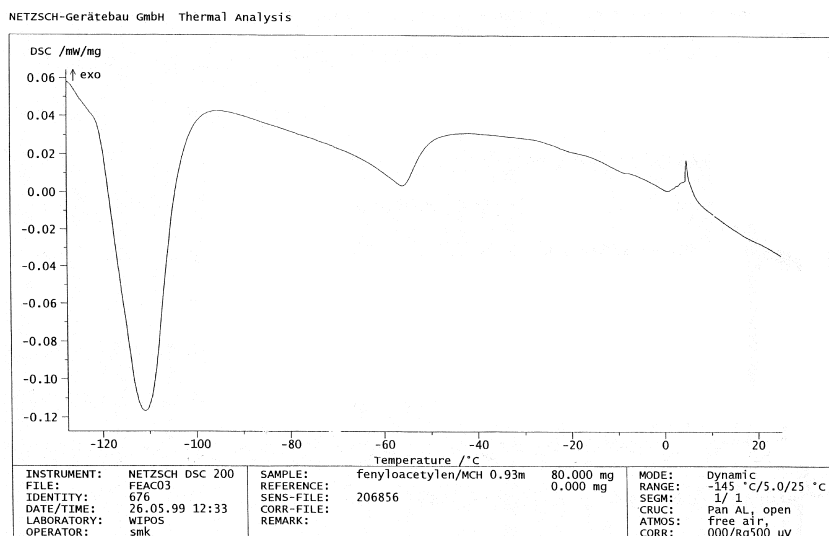
Fig. 9. Differential scanning calorimeter scan of neat methylcyclohexane.

acetonitrile (Figs. 7 and 8) with the DSC traces for methylcyclohexane and PA in methylcyclohexane shown in Figs. 9 and 10. We can see that comparison between the DSC scans for PA in acetonitrile and in neat acetonitrile provides an evidence on the strong coupling between PA and acetonitrile molecules. The comparison between the DSC scans of PA in methyl-cyclohexane and neat methylcyclohexane gives quite a different pattern of behaviour. The diagram for neat methylcyclohexane shows a melting transition starting at 120 K, which does not change in PA solution, in contrast to PA in acetonitrile. The DSC scan for PA in methylcyclohexane shows additional phase transition at around 220 K. Methylcyclohexane, in contrast to acetonitrile, does not form H-bonds with PA and this source of the coupling with solvent disappears. The DSC results for PA in benzene show the similar pattern of behaviour as observed for PA



Fig. 10. Differential scanning calorimeter scan of phenylacetylene in methylcyclohexane (0.93 mol/dm$^3$).

in acetonitrile. The melting transition, which starts for neat benzene at 279 K is strongly depressed in PA solution to 233 K, and again as in acetonitrile two strong DSC melting-like peaks are observed in contrast to one peak in neat benzene, suggesting a strong coupling with the solvent, which is likely due to H-bonds between PA protons and $\pi$-electrons of benzene ring.

In the view of these results, the transition at 200 K (Fig. 8) ascribed to the plastic crystal–glassy plastic crystal transition is likely to represent the transition from plastic structure ordered by H-bond interactions between PA protons and $\pi$-electrons of the triple bond C≡N of acetonitrile and/or C≡C of PA to more disordered glassy plastic crystal, in which many H-bonds were broken due to increasing thermal fluctuations. However, the phase existing between 200 and 218 K, called here the glassy plastic crystal, does not seem to be characterised by the macroscopic orientational isotropy. The orientational isotropy is reached above the transition at 218 K ascribed to glassy plastic crystal–isotropic liquid phase transition. The information about orientational isotropy has been obtained from the VV–VH polarization Raman measurements. We have found that the depolarization ratio, which depends on the symmetry of the vibration and in isotropic environments should be constant, changes drastically at 218 K. The DSC scans for PA in methylcyclohexane (Fig. 10) may be interpreted consistently as a melting transition at 120 K from the crystal to the glassy plastic crystal followed by the glassy plastic–isotropic liquid transition at 220 K. Also in this case, similary to PA in acetonitrile, the glassy plastic crystal phase is not orientationally isotropic and has anisotropic alignment typical for the liquid crystal phase.

The first observation that one makes when confronting the results obtained by the DSC method and the Raman spectra for different molecular solvents is that there is an evident correlation between the vibrational substructure and the strength of the coupling with solvent revealed from the DSC results. In this context, it is conceivable that the similar structure persists in the liquid phase although the components are no longer resolvable because of bandbroadening due to vibrational dephasing at higher temperatures. Indeed, it is worth pointing out that the $\nu_s$(C≡C) band of PA in the isotropic liquid phase is asymmet-

ric on the low frequency side and it may illustrate the convolution of the bands, which represents the H-bonded and unbounded PA oscillators.

In view of these results on solvent and concentration effects as well as the cooling rate dependence we first need to ask for the origin of splitting. In general, the splitting may depend on the following factors:

(1) A factor group splitting [8] of the $\nu_s$(C≡C) vibrational mode of PA.

(2) A factor group splitting of the solute/solvent modes of lower frequency coupled to the $\nu_s$(C≡C) mode of PA.

(3) Splitting due to tunneling through periodic barrier for internal rotations [9–11] or exchange tunneling in H-bonded systems [12–16].

(4) The interaction between the upper state of an allowed transition and a near resonant optically inactive state [17].

(5) Shift of vibrational components of the $\nu_s$(C≡C) mode of PA due to the coupling with the lower frequency modes of acetonitrile and/or PA.

(6) Coexistence between crystalline and amorphous mesophases.

The factor group splitting of the $\nu_s$(C≡C) mode of PA would be appealing as it is typical for crystal and absent in glasses and it would explain the three subbands of PA in acetonitrile or benzene (Figs. 2, 3, 5 and 6) and a single peak in methylcyclohexane (Figs. 1 and 4). To determine if the factor group splitting leads to the observed changes we have performed the studies on the band shape analysis upon isotopic substitution. We shall defer an analysis of the deuteration effect on the Raman spectra for these systems to another paper [18], but we would like to point out the effectiveness of isotopic mixtures studies to determining the nature of the splitting as the multiplet structure of nonsubstituted crystal should be perturbed severely in the isotopically mixed crystals when the factor group splitting plays a crucial role.

Anticipating the full presentation of the deuteration results, we have found that the substructure of the $\nu_s$(C≡C) band does not change with isotopic substitution both for PA and PA–d$_6$ and the relative intensities of the components remain similar in the full concentration range from the mole fraction of deuterated PA $x = 0.0$ to $x = 1.0$. The similarity

between the spectra as a function of the isotopic substitution in terms of the peak intensities makes abundantly clear that the origin of the splitting does not come from the factor group splitting of the $\nu_s(C\equiv C)$ vibration.

The interconversion tunneling due to exchange of proton involved in H-bond between two phenylacetylene molecules does not seem to affect the Raman spectra. The tunneling frequency for acetylene was found to be 2.1 GHz $(0.07 \text{ cm}^{-1})$ [12], which is much lower than the resolution of our experiment $(0.5 \text{ cm}^{-1})$. For phenylacetylene, which has a significantly larger moment of inertia than acetylene, the splitting due to tunneling seems to be even more negligible as this effect comes from the synchronous rotation of both PA units during the tunneling process. Moreover, the deuteration of PA leads to increasing, instead of decreasing, the distances between the vibrational peaks of the $\nu_s(C\equiv C)$ vibration from about 5 cm$^{-1}$ for PA to 6 cm$^{-1}$ for PA–d$_6$. The splitting of the $\nu_s(C\equiv C)$ vibration due to tunneling through periodic barrier for internal rotations of the phenyl ring in PA molecule around the C$_{2v}$ axis can be eliminated on the same basis.

The intramolecular interaction between the upper state of an allowed transition and a near resonant optically inactive state is not representative for this case because the results show evidently intermolecular character of interactions as the splitting changes with solvent and concentration.

To learn more about the origin of the substructure of vibrational bands in different solvents and about mechanisms of vibrational dynamics illustrated by the band shapes and widths, it would be very valuable studying the response of the solvent to the interactions with PA and to perform temperature-dependent studies. They may help to find if the processes responsible for the observed components are thermally activated and to estimate the activation energies governing vibrational dynamics of each component of PA as well as the vibrations of the solvent which are supposed to be coupled to the solute.

We have performed the temperature-dependent measurements both for PA and solvent vibrational modes and the results will be presented in a subsequent paper [19]. Anticipating our results we have found that the $\nu_s(C\equiv C)$ vibration of PA in aceto-

nitrile shows approximately Arrhenius behaviour with a thermal activation energy of $310 \pm 108$, $190 \pm 74$, and $112 \pm 34$ cm$^{-1}$ for the peaks at 2105, 2110, and 2116 cm$^{-1}$, respectively. The activation energy for the peak at 2105 cm$^{-1}$ cover the range of the $\nu_{16a}(B_2)$ (boat) vibration of the phenyl ring in PA at 349 cm$^{-1}$ [20] and the bending mode $\nu_8(E)(C–C\equiv N)$ at 375 cm$^{-1}$ in acetonitrile [21], respectively. The activation energies for higher frequency peaks cover the range of translational and librational optic phonons at much lower energies than the $\nu_8$ and $\nu_{16}$ modes. The vibrations, which we have obtained to be preferentially coupled to phenylacetylene, serve to emphasise the striking connection with our earlier suggestion about the origin of the components observed in the low temperature spectra of PA. Clearly, both $\nu_8$ and $\nu_{16}$ vibrations may strongly perturb the T-shaped geometry of the H-bond complex, although the influence of the large-amplitude bending vibration $\nu_8$ of acetonitrile seems to be dominant in this kind of the coupling.

The picture that emerges from the analysis to this point is as follows. The highest frequency peak at about 2116 cm$^{-1}$ observed in all the solvents represents the 'free' band of the $\nu_s(C\equiv C)$ stretching mode of PA which is not involved in H-bond complex. The peaks at about and 2110 cm$^{-1}$ come from the coupling with the modes in the range 300–400 cm$^{-1}$ ($\nu_8$ of acetonitrile, $\nu_{16a}$ of PA, $\nu_{16}$ of benzene) and 100–200 cm$^{-1}$ (C$\equiv$C–C bending mode at 140 cm$^{-1}$ for PA, the low frequency translational and librational phonons of acetonitrile and benzene), respectively.

The nature of this coupling seems to be dominated by the H-bond interactions. It was found [22,23] that the profile of the H-bond complex is a set of lines peaked at:

$$\omega_{\gamma\alpha} = \omega_0 - 2\alpha_0^2\omega_{00} + (\gamma - \alpha)\omega_{00}, \qquad (4)$$

where $\omega_0$ is the angular frequency of the free species, $\omega_{00}$ represents the low-frequency mode coupled with the $\omega_0$ oscillator through H-bond, $\alpha_0$ is the strength of the coupling, $\gamma$, $\alpha$ are the vibrational quantum numbers of the $\omega_{00}$ oscillator. At low temperatures the second term in Eq. (4) can be neglected. We can estimate the magnitude of $\alpha_0$ from Eq. (4) assuming that $\omega_0 = 2116$ cm$^{-1}$, $\omega_{00} = 375$ cm$^{-1}$($\nu_8$ of acetonitrile), and $\omega_{\gamma\alpha} = 2105$ cm$^{-1}$, which gives

$\alpha_0 = -0.12$. (For comparison, we have found [23] $\alpha_0 = -1.2$ for methanol in $CCl_4$ and $\alpha_0 = -1.33$ for HF-dimethylether.) Using $\alpha_0 = -0.12$ and the activation energy obtained from the Arrhenius plot of $\omega_{00} = 190$ cm$^{-1}$ for the second component, the position of the peak in the middle at 2110.4 cm$^{-1}$ is correctly predicted with Eq. (4).

The same physical mechanism is able to explain the other features of the Raman spectra presented in this paper:

(i) intensity decrease of the PA peak at 2105 cm$^{-1}$ observed in acetonitrile and benzene solutions when PA concentration increases (Figs. 5 and 6) as the number of H-bond complexes in which acetonitrile or benzene are involved decreases,

(ii) a single peak at 2116 cm$^{-1}$ observed for PA in methylcyclohexane (Figs. 1 and 4) as H-bond interaction is absent in this system.

However, in the framework of this interpretation it is hard to understand why the Raman spectra depend on the cooling rate (compare Fig. 1 with Fig. 4, Fig. 2 with Fig. 5, Fig. 3 with Fig. 6). This behaviour can be understood in terms of the structure of glassy and crystalline materials, which are formed upon annealing. When rapid cooling occurs to a temperature at which the crystalline state is expected to be more stable, it may happen that molecular movement is too sluggish and awkward to take up a crystalline conformation. Therefore the random arrangement characteristic of liquid persists down to temperatures at which the viscosity is too high that the material is considered to be solid and the glassy state is generated. However, the reverse situations have also been reported [1], when glassy states can be generated during very slow cooling. The changes of the relative intensities of the components at 2105, 2110 and 2116 cm$^{-1}$ in acetonitrile and benzene as well as in neat PA may illustrate the different degree of crystallinity of the sample and the different contribution from phonons of the crystal network to vibrational dynamics. The peak at 2105 cm$^{-1}$, which represents in our interpretation the coupling with the relatively high frequency modes is especially sensitive to the cooling rate.

This interpretation is not in contradiction to that based on H-bond coupling. Clearly, it is good to remember that the intensity of subpeaks in H-bond complexes depends on the damping parameter $\Gamma$

[22,23] which reflects the strength of the coupling between the solvent mode involved in H-bond and the bath. In this case, the parameter $\Gamma$ describes the influence of the bath on the $\nu_s(C\equiv C)$ vibrational mode of PA exerted indirectly through disturbing the H-bond bridge motion (in which the $\nu_8$ of acetonitrile, $\nu_{16a}$ of PA, $\nu_{16}$ of benzene are engaged). For perfectly isolated H-bond complex the parameter $\Gamma$ is equal to zero. In fact, the environment of the H-bond leads to non-zero $\Gamma$ magnitudes. The environments are different in crystal and glassy structures resulting in changes of the damping parameter, which modifies intensities, shapes, and even peak positions. Additionally, we should remember that with increasing PA concentration the competition between PA–solvent and PA–PA becomes more and more important. Moreover, for higher PA concentrations, one may expect two kind of $\nu_s(C\equiv C)$ oscillators: for PA molecules being proton donors and proton acceptors.

## 4. Conclusions

We have presented Raman spectra of the $\nu_s(C\equiv C)$ stretching mode of phenylacetylene (PA) dissolved in different solvents: methylcyclohexane, acetonitrile and benzene in frozen matrices at 77 K as a function of concentration, which were compared with the spectra in the liquid phase. The optical measurements were complemented by the differential scanning calorimetry (DSC) scans.

One of the goals of the paper was to identify the mesophases of phenylacetylene in solutions. We have found a glass-like transition at 183 K ascribed to the crystal–plastic crystal transition and a solid–solid transition at 200 K, which melts the structure ordered by H-bond interactions (plastic crystal) leading to the disordered structure (glassy plastic crystal). The transition at 218 K represents the transformation from the glassy plastic crystal to isotropic liquid. In methylcyclohexane a melting transition from a solid to plastic phase starts at 120 K, and does not change in PA solution in contrast to PA in acetonitrile. The DSC scan for PA in methylcyclohexane shows additional phase transition at about 220 K, which we ascribe to the glassy plastic crystal–isotropic liquid transition. The plastic crystal phase both for PA in acetonitrile and methylcyclohexane is characterised

by the macroscopic orientational anisotropy, which is typical for liquid crystals. We have found that the morphology of the PA solutions depends on the rate of cooling. Slow quenching leads to more glass-like behaviour whereas rapid cooling generates crystal-like behaviour for PA in acetonitrile and methylcyclohexane. The situation seems to be reversed for PA in benzene – slow cooling leads to more crystalline structure.

Raman spectra of PA in solutions at low temperature are very sensitive to the details of intermolecular interactions and consistent with the DSC results. We have discussed the origin of the splitting observed for the $\nu_s(C{\equiv}C)$ stretching mode of phenylacetylene (PA). We have found that H-bond interactions are responsible for the observed substructure in the vibrational spectra. This finding gives the opportunity for studying H-bond complexes in the full temperatures range going from isotropic liquids to glassy or crystalline solids. These results may provide deeper understanding of mechanisms of vibrational dephasing and band broadening in H-bonded systems as well as a correlation with phase transitions. At the moment it is too early to outline a complete picture which will be able to correlate the vibrational dynamics with the specific phase transitions. However, it is already clear that Raman experiments provide an excellent method of structure monitoring for the stretching mode $\nu_s(C{\equiv}C)$ of PA in solutions on going from isotropic liquids at room temperature to solid state phases at low temperature. We hope, it will help in the future to answer the basic questions about ordering and alignment during the phase transition.

## Acknowledgements

## References

[1] C.A. Angell, P.H. Poole, J. Shao, Nuovo Cimento 16 (1994) 993.
[2] G.P. Crawford, S. Žumer, Liquid Crystals in Complex Geometries, Taylor & Francis, London, 1996.
[3] F.G. Dijkman, J.H. van Maas, Appl. Spectrosc. 30 (1976) 545.
[4] H. Abramczyk, G. Waliszewska, B. Brożek, J. Phys. Chem. (1999, submitted for publication).
[5] H. Abramczyk, G. Waliszewska, M. Kołodziejski, J. Phys. Chem 102 (1998) 1918.
[6] H. Abramczyk, G. Waliszewska, M. Kołodziejski, J. Phys. Chem 102 (1998) 7765.
[7] W.G. Rothschild, Dynamics of Molecular Liquids, Wiley, New York, 1984, pp. 100, 261.
[8] D.D. Dlott, Laser Spectroscopy of Solids II, in: W.M. Yen (Ed.), Springer, Berlin, 1989, p. 167.
[9] T.P. Das, J. Chem. Phys. 25 (1956) 896.
[10] T.P. Das, J. Chem. Phys. 27 (1957) 763.
[11] C.H. Townes, A.L. Schawlow, Microwave Spectroscopy, McGraw-Hill, New York, 1955.
[12] G.T. Fraser, J. Chem. Phys. 90 (1989) 2097.
[13] T.R. Dyke, B.J. Howard, W. Klemplerer, J. Chem. Phys. 56 (1972) 2442.
[14] A.S. Pine, W.J. Lafferty, J. Chem. Phys. 78 (1983) 2154.
[15] G.A. Blake, K.L. Busarow, R.C. Cohen, K.B. Laughlin, Y.T. Lee, R.J. Saykally, J. Chem. Phys. 89 (1988) 6577.
[16] A.S. Pine, W.J. Lafferty, B.J. Howard, J. Chem. Phys. 81 (1984) 2939.
[17] R.E. Miller, Acc. Chem. Res. 23 (1990) 10.
[18] H. Abramczyk, B. Brożek, G. Waliszewska (in preparation).
[19] H. Abramczyk, B. Brożek, Chemical Physics (1999), in press.
[20] A. Shimojima, H. Takahashi, J. Phys. Chem. 97 (1993) 9103.
[21] J. Yarwood, in: J. Yarwood (Ed.), Spectroscopy and Structure of Molecular Complexes, Plenum, New York 1973, p. 142.
[22] H. Abramczyk, Chem. Phys. 144 (1990) 305.
[23] H. Abramczyk, Chem. Phys. 144 (1990) 319.